AMERICAN SOCIETY FOR MICROBIOLOGY | Journal of Bacteriology®

RESEARCH ARTICLE

Mutational Analysis of *Vibrio fischeri* c-di-GMP-Modulating Genes Reveals Complex Regulation of Motility

Prerana Shrestha,[a] Ali Razvi,[a]* Brittany L. Fung,[a] Steven J. Eichinger,[a]§ Karen L. Visick[a]

[a]Loyola University Chicago, Maywood, Illinois, USA

ABSTRACT The symbiont *Vibrio fischeri* uses motility to colonize its host. In numerous bacterial species, motility is negatively controlled by cyclic-di-GMP (c-di-GMP), which is produced by diguanylate cyclases (DGCs) with GGDEF domains and degraded by phosphodiesterases with either EAL or HD-GYP domains. To begin to decode the functions of the 50 *Vibrio fischeri* genes with GGDEF, EAL, and/or HD-GYP domains, we deleted each gene and assessed each mutant's migration through tryptone broth salt (TBS) soft agar medium containing or lacking magnesium (Mg) and calcium (Ca), which are known to influence *V. fischeri* motility. We identified 6, 13, and 16 mutants with altered migration in TBS-Mg, TBS, and TBS-Ca soft agar, respectively, a result that underscores the importance of medium conditions in assessing gene function. A biosensor-based assay revealed that Mg and Ca affected c-di-GMP levels negatively and positively, respectively; the severe decrease in c-di-GMP caused by Mg addition correlates with its strong positive impact on bacterial migration. A mutant defective for *VF_0494*, a homolog of *V. cholerae rocS*, exhibited a severe defect in migration across all conditions. Motility of a *VF_1603 VF_2480* double mutant was also severely defective and could be restored by expression of "c-di-GMP-blind" alleles of master flagellar regulator *flrA*. Together, this work sheds light on the genes and conditions that influence c-di-GMP-mediated control over motility in *V. fischeri* and provides a foundation for (i) assessing roles of putative c-di-GMP-binding proteins, (ii) evaluating other c-di-GMP-dependent phenotypes in *V. fischeri*, (iii) uncovering potential redundancy, and (iv) deciphering signal transduction mechanisms.

IMPORTANCE Critical bacterial processes, including motility, are influenced by c-di-GMP, which is controlled by environment-responsive synthetic and degradative enzymes. Because bacteria such as *Vibrio fischeri* use motility to colonize their hosts, understanding the roles of c-di-GMP-modulating enzymes in controlling motility has the potential to inform on microbe-host interactions. We leveraged recent advances in genetic manipulation to generate 50 mutants defective for putative c-di-GMP synthetic and degradative enzymes. We then assessed the consequences on motility, manipulating levels of magnesium and calcium, which inversely influenced motility and levels of c-di-GMP. Distinct subsets of the 50 genes were required under the different conditions. Our data thus provide needed insight into the functions of these enzymes and environmental factors that influence them.

KEYWORDS *Vibrio fischeri*, c-di-GMP, flagellar motility, reverse genetic analysis, signal transduction

The second messenger cyclic diguanylate (c-di-GMP) is a key regulator that influences a wide array of pathways, including motility, biofilm formation, and virulence (1–3). Central to c-di-GMP signaling are enzymes, diguanylate cyclases (DGCs) and phosphodiesterases (PDEs), that synthesize and degrade this small molecule, respectively, often in response to environmental signals. Completing the signal transduction

Editor Anke Becker, Philipps University Marburg

Address correspondence to Karen L. Visick, kvisick@luc.edu.

*Present address: Ali Razvi, Abbott Labs, Abbott Park, Illinois, USA.

§Present address: Steven J. Eichinger, Department of Microbiology, University of Illinois at Urbana-Champaign, Urbana, Illinois, USA.

The authors declare no conflict of interest.

Received 23 March 2022
Accepted 4 June 2022
Published 27 June 2022

pathway, c-di-GMP binds proteins or RNA, thus stimulating or inhibiting a downstream response.

Bioinformatics and biochemical work have revealed key domains and motifs that allow these enzymes and regulators to carry out their functions (4–8). Functional DGCs generally contain GGDEF domains with a GG(D/E)EF active site, although other variations in this motif may be permissive for function (e.g., reference 9). A subset of DGCs also contains an I-site (inhibitory site), RxxD, that is positioned five residues upstream of the GG(D/E)EF motif; c-di-GMP binding at this position causes feedback inhibition of the DGC (10). Two general classes of PDEs are known, those that contain an EAL domain with an ExLxR motif and those that contain an HD-GYP domain with HD and GYP motifs (4, 11). Some proteins contain both GGDEF and EAL domains and may have dual function, exhibiting both DGC and PDE activity and switching those activities in response to a signal(s). Other GGDEF- and/or EAL-containing proteins are degenerate, lacking clear GGDEF or EAL motifs and/or having incomplete domains. In some cases, degenerate proteins that lack enzymatic activity retain the ability to bind c-di-GMP, thus maintaining a role in a signaling pathway. In particular, I-site-containing degenerate DGCs can bind c-di-GMP. In addition to degenerate enzymes, many other types of proteins appear competent to bind c-di-GMP, including a class of proteins that contain the PilZ domain (12). Finally, many GGDEF, EAL, and/or HD-GYP proteins also contain predicted sensory domains that likely influence their activities.

Some bacteria possess no or only a few proteins that control c-di-GMP levels, while others contain numerous such enzymes. In general, *Vibrio* species encode large numbers of these proteins, with the pathogens *Vibrio cholerae*, *Vibrio parahaemolyticus*, and *Vibrio vulnificus* predicted to contain 62, 62, and 92 DGC/PDE enzymes, respectively (https://www.ncbi.nlm.nih.gov/Complete_Genomes/c-di-GMP.html) (2, 5, 12, 13). The symbiont *V. fischeri* encodes 50 proteins with GGDEF/EAL/HD-GYP annotations (14–16). The large numbers of these proteins suggest that c-di-GMP signaling provides key advantages to this species.

V. fischeri serves as an important model for a variety of biological phenomena, including bioluminescence, biofilm formation, and symbiosis. This marine bacterium forms an exclusive symbiosis with *Euprymna scolopes*, a Hawaiian squid (reviewed in references 17 and 18). By colonizing the squid, *V. fischeri* gains nutrients and a protected environment in exchange for its bioluminescence, which *E. scolopes* uses to evade predation. Newly hatched, uncolonized juvenile squid are colonized by *V. fischeri* present in the surrounding seawater in a series of events that include those that are known to be affected by c-di-GMP signaling, biofilm formation, and motility. Notably, mutants defective for biofilm formation or motility are deficient in colonizing squid.

Because of its importance in squid colonization and the ease with which it can be studied, motility of *V. fischeri* has been probed in a number of studies (e.g., references 19–22). In laboratory culture, *V. fischeri* motility is affected by the presence of the cations magnesium (Mg) and calcium (Ca) (23). Addition of 35 mM Mg (the amount present in seawater) permits *V. fischeri* to migrate through a soft agar medium more rapidly than in its absence. Mg exerts that effect by increasing the number of flagella per cell (23). The impact of Ca varies, dependent on the concentration. At concentrations of 10 mM and below, Ca supplementation increases bacterial migration through soft agar, albeit to a lesser extent than that caused by Mg (23). At higher concentrations, notably 40 mM and above, Ca exerts a negative effect on migration. Investigation into the role of Mg in promoting *V. fischeri* motility led to the identification of MifA (VF_0989) and MifB (VF_A0959), two DGCs that contributed to the poor migration of *V. fischeri* in the absence of Mg (24). More recently, the DGC CasA (encoded by *VF_1639*) was shown to control the response to high levels of Ca: mutation of *casA* permitted *V. fischeri* to migrate to the same extent that occurred in the absence of high calcium, rather than exhibiting the reduced migration of the wild-type strain (25). Together, these studies revealed the importance of cations in controlling *V. fischeri* motility and identified roles for three specific DGCs in motility under different conditions.

TABLE 1 Putative DGCs

Protein and motif information[a]				Migration results[b]		
Protein	RxxD	GG(D/E)EF	Vc homolog	TBS-Mg	TBS	TBS-Ca
VF_0596		**S**GEEF	VC_0900 (CdgG)	−	−	−
VF_0989 (*mifA*)	RSID	GGEEF			+	+
VF_1200		GGDEF			+	+
VF_1245		GGEEF				
VF_1350	**K**END	GGEEF				
VF_1515		GGDEF	VC_1376 (CdgM)			
VF_1561	**K**STD	GGEEF	VC_1185			
VF_1639 (CasA)	RDSD	GGEEF	VC_1104 (CdgK)			+
VF_2261	RETD	GGEEF			+	
VF_2362	RQSD	GGDEF				
VF_A0056	RSRD	GGDEF				
VF_A0057	**F**END	**S**GDEF				
VF_A0152	**E**SDD	GGDEF				
VF_A0155	**N**QDD	GGDEF				+
VF_A0276		GGEEF				+
VF_A0323		GGDEF				
VF_A0342	RVND	GGEEF				
VF_A0343	RGDD	GGEEF				
VF_A0368		GGEEF			−	
VF_A0381		GGEEF			+	+
VF_A0398		GGEEF				
VF_A0476		GGDEF				−
VF_A0567	RAND	**A**GDEF				
VF_A0692		GGEEF				
VF_A0796	RNTD	GGEEF				
VF_A0959		GGDEF		+	+	+
VF_A0976		GGDEF				−
VF_A1012	RKTD	GGEEF				

[a]Listed are the *V. fischeri* protein, the putative I-site (RxxD), and/or the GGDEF motif (the former 5 bp upstream of GGDEF motif), with residues that depart from the consensus shown in bold and the *V. cholerae* homolog (see Table 5 for detailed information).
[b]Symbols reflect migration results of the mutant relative to those the wild-type parent, as follows: −, decreased and +, increased.

Here, we take a global approach to probing the functions of putative DGC and PDE enzymes in the physiology of *V. fischeri*, focusing specifically on bacterial motility using the sensitive soft agar migration assay. We leveraged recent advances in tools for rapid genetic manipulation of *V. fischeri* (26) to generate mutations in each of the 50 genes encoding proteins with GGDEF, EAL, and HY-GYP domains in wild-type squid symbiont strain ES114. These studies revealed putative DGCs and PDEs with significant roles in controlling *V. fischeri* motility. Furthermore, by manipulating Mg and Ca levels to alter environmental conditions, we uncovered additional c-di-GMP regulators responsive to particular conditions. Finally, our studies demonstrated a conservation in function between *V. fischeri* and *V. cholerae* for certain DGCs and PDEs.

RESULTS AND DISCUSSION

Functional grouping of 50 c-di-GMP-related genes in *V. fischeri*. *V. fischeri* strain ES114, a symbiont of the squid *E. scolopes*, contains 50 genes encoding GGDEF, EAL, or HY-GYP proteins in its genome (14–16). To begin characterizing this extensive c-di-GMP regulatory network, we used bioinformatics tools to identify putative associated sensory domains (see Fig. S1 in the supplemental material), to assess whether each may be catalytically active or degenerate (based on the conservation of motifs and the presence/absence of intact domains) (Table 1 to 4), and to predict where each may be localized in the cell (Fig. S2). We also compared these enzymes to those encoded by *V. cholerae* (27), whose extensive regulatory network has been assessed previously (e.g., reference 28) (Table 5). These analyses permitted us to classify these proteins into

TABLE 2 Putative PDEs[a]

Protein and motif information[a]			Migration results[b]		
Protein	**ExLxR/HD-GYP**	**Vc homolog**	**TBS-Mg**	**TBS**	**TBS-Ca**
VF_0087	ECLMR	VC_0130 (CpdA)		−	
VF_0091	EALIR	VC_2750			
VF_1603	ELLFR	VC_1851	−	−	−
VF_2480	ELLFR	VC_0137 (CdgJ)	−	−	−
VF_A0344	EVLAR				
VF_A0526	EVLLR		−	−	−
VF_A0551	EALLR	VC_A0536			
VF_A0706	EALLR				
VF_A0879	EALSR				
VF_A1014 (PdeV)	EALIR				
VF_A1038 (BinA)	EALLR	CdgC			
VF_A1076	EALLR				
VF_1367	HD-GY				
VF_A0506	HD-GYP				

[a]Listed are the *V. fischeri* protein, the putative ExLxR or HD-GYP motif, and the *V. cholerae* homolog (see Table 5 for detailed information). VF_0087, VF_0091, and VF_A1038 have apparently degenerate GGDEF motifs, as follows, respectively: GIAEW, GGAEF, and GSSDI. VF_1367 lacks the P of the HD-GYP motif.
[b]Symbols reflect migration results of the mutant relative to those the wild-type parent, as follows: −, decreased.

four putative functional groups: (i) DGCs, (ii) PDEs, (iii) dual-function DGC/PDEs, and (iv) nonenzymatic, putative c-di-GMP-binding proteins.

Group 1 (Table 1) encompasses 28 putative DGCs that contain a conserved GGDEF domain with a fully or largely conserved GG(D/E)EF motif. We included in this group three proteins that contain a noncanonical residue in the first amino acid of the GGDEF motif. One contains an alanine in that position (VF_A0567), while two contain a serine (VF_0596 and VF_A0057). Functional DGCs with these substitutions have been reported previously. For example, *V. cholerae* VC_A0965 contains an alanine in that position, yet it is a fully functional DGC (9), while *Pectobacterium atrosepticum* expresses an active DGC that contains a serine (29). However, CdgG (VC_0900), a homolog of VF_0596 (Table 5) that contains a serine instead of glycine in that location, lacks DGC activity and inhibits rather than promotes c-di-GMP-dependent phenotypes in *V. cholerae* (30); thus, the inclusion of this or the other two *V. fischeri* enzymes with noncanonical GGDEF motifs in this class may need to be revisited at a later time. In addition to VF_0596, three other putative DGCs exhibit significant similarity to *V. cholerae* proteins, VF_1515 (VC_1376, CdgM), VF_1561 (VC_1185), and CasA (VF_1639; VC_1104, CdgK) (Table 5). Finally, 10 have putative I-sites (RxxD) that are conserved, while 5 others contain a properly positioned D but another residue in place of the R, and the remaining 13 lack a putative I-site.

Group 2 (Table 2) includes 14 putative phosphodiesterase proteins. Of these, 12 have a conserved EAL domain with a fully conserved ExLxR motif; three of these also contain a degenerate GGDEF domain or motif, making them unlikely to be catalytically active as DGCs. Five of the EAL-domain-containing proteins are similar to those found

TABLE 3 Putative dual DGC/PDE proteins

Protein and motif information[a]					Migration results[b]		
Protein	**RxxD[a]**	**GGDEF**	**ExLxR**	**Vc homolog**	**TBS-Mg**	**TBS**	**TBS-Ca**
VF_0094		GGDEF	EALIR	VC2750			−
VF_0494		GGDEF	EALVR	VC_0653 (RocS)	−	−	−
VF_0985		GGDEF	EVLSR			+	
VF_A0244	RKED	GGDEF	EALIR				
VF_A0475	RKED	GGDEF	EALLR				

[a]Listed are the *V. fischeri* protein, the putative I-site (RxxD) and/or GGDEF motif (the former 5 bp upstream of GGDEF motif), the ExLxR motif, and the *V. cholerae* homolog (see Table 5 for detailed information).
[b]Symbols reflect migration results of the mutant relative to those the wild-type parent, as follows: −, decreased and +, increased.

TABLE 4 Putative nonenzymatic GGDEF and EAL proteins

Protein and motif information[a]				Migration results[b]		
Protein	**GG(D/E)EF**	**ExLxR**	**Vc homolog**	**TBS-Mg**	**TBS**	**TBS-Ca**
VF_0355 (MshH/CsrD)	**YQSD**F	EL**F**SR	VC_0398 (MshH)			−
VF_A0216		**QVSPH**				
VF_A1166 (LapD)	**NSS**EF	EV**F**SA	VC_A1082 (LapD)			

[a]Listed are the *V. fischeri* protein, the residues that align with the GGDEF and/or ExLxR motif, and the *V. cholerae* homolog (see Table 5 for detailed information). The residues that depart from consensus are shown in bold.
[b]Colors reflect migration results of the mutant relative to the wild-type parent, as follows: −, decreased.

in *V. cholerae* (Table 5): VF_0087 (VC_0130, CpdA), VF_0091 (VC_2750), VF_1603 (VC_1851), VF_2480 (VC_0137, CdgJ), and VF_A0551 (VC_A0536). Of note, both VF_0091 and, below in group 3, VF_0094 are similar to VC_2750 and to each other; while VF_0091 contains a putative GGDEF domain, it lacks an intact GGDEF motif, containing instead a GGAEF motif that is expected to lack DGC activity. VF_1603 and VF_2480 also exhibit substantial similarity to each other; in this case, each is most similar to a distinct *V. cholerae* protein (VC_1851 and VC_0137, respectively) (Table 5). Also included in this group are two proteins that contain an HD-GYP domain. VF_A0506 contains HD and GYP amino acids with spacing similar to that found in other HD-GYP proteins (31), while VF_1367 lacks the P of the GYP portion of the HD-GYP motif.

Group 3 (Table 3) includes five proteins that contain both GGDEF and EAL domains with intact motifs, supporting their assignment as putative dual-function DGC/PDEs; two of these also contain intact I-sites. VF_0094 and VF_0494 exhibit significant sequence similarity to *V. cholerae* proteins VC_2750 and VC_0653 (RocS [32]), respectively (Table 5).

Finally, group 4 (Table 4) includes three proteins with degenerate domains and/or motifs, suggesting that these proteins lack enzymatic activity but may function as c-di-GMP-binding proteins. One of these is VF_A1166, or LapD, a homolog of the *Pseudomonas* LapD protein that binds c-di-GMP, permitting it to sequester the LapG protease responsible for cleaving a surface adhesin (reviewed in reference 33); VF_A1166/LapD appears to function in the same manner (34), as does its *V. cholerae* homolog, VC_A1082 (35). Another is VF_0355 or MshH (CsrD), which is a homolog of *V. cholerae* VC_0398 (Table 5);

TABLE 5 Comparisons of *V. fischeri* proteins with *V. cholerae* proteins

Protein					
V. fischeri	***V. cholerae***	**Expect**	**Identity (%)**	**Similarity (%)**	**Gaps (%)**
VF_0087	VC_0130 (CpdA)	0	359/829 (43%)	511/829 (61%)	3/829 (0%)
VF_0091	VC_2750	0	295/806 (37%)	474/806 (58%)	16/806 (1%)
VF_0094	VC_2750	0	391/846 (46%)	564/846 (66%)	13/846 (1%)
VF_0355	VC_0398 (MshH)	0	329/642 (51%)	453/642 (70%)	2/642 (0%)
VF_0494	VC_0653 (RocS)	0	439/676 (65%)	546/676 (80%)	5/676 (0%)
VF_0596	VC_0900 (CdgG)	4.00E−135	212/513 (41%)	336/513 (65%)	2/513 (0%)
VF_1515	VC_1376 (CdgM) (AdrA_2)	4.00E−117	186/478 (39%)	288/478 (60%)	3/478 (0%)
VF_1561	VC_1185	9.00E−129	178/431 (41%)	275/431 (63%)	5/431 (1%)
VF_1603	VC_1851	5.00E−175	233/397 (59%)	302/397 (76%)	0/397 (0%)
	VC_0137 (CdgJ)	4.00E−126	190/409 (46%)	274/409 (66%)	12/409 (2%)
VF_1639 (CasA)	VC_1104 (CdgK)	2.00E−87	145/492 (29%)	266/492 (54%)	11/492 (2%)
VF_2480	VC_0137 (CdgJ)	1.00E−150	208/404 (51%)	296/404 (73%)	2/404 (0%)
	VC_1851	1.00E−118	178/403 (44%)	267/403 (66%)	4/403 (0%)
VF_A0551	VC_A0536	7.00E−68	113/255 (44%)	157/255 (61%)	3/255 (1%)
VF_A1038 (BinA)	VC_A0785 (CdgC)	0	279/618 (45%)	407/618 (65%)	7/618 (1%)
VF_A1166 (LapD)	VC_A1082 (LapD)	3.00E−161	216/379 (57%)	286/379 (75%)	0/379 (0%)
V. fischeri protein 1	*V. fischeri* protein 2				
VF_0091	VF_0094	0	335/824 (41%)	512/824 (62%)	17/824 (2%)
VF_1603	VF_2480	1.00E−130	186/402 (46%)	278/402 (69%)	4/402 (0%)
VF_A0342	VF_A0343	2.00E−85	156/434 (36%)	246/434 (56%)	16/434 (3%)

in *V. cholerae*, this protein functions to inhibit biofilm formation under specific conditions (36). The last protein in this group is VF_A0216, which contains a response regulator receiver (REC) domain and a degenerate EAL domain.

Our list of 50 proteins and their grouping into functional categories differs in three ways from that proposed by Galperin et al. (https://www.ncbi.nlm.nih.gov/Complete_Genomes/c-di-GMP.html) (2, 5, 12, 13). First, due to errors in the original sequence of the ES114 genome that were later uncovered (14, 15), the genes encoding VF_A0242, VF_A0243, and VF_A0244 were resolved into a single gene, *VF_A0244*, which encodes a dual GGDEF/EAL protein. Second, protein VF_A0477, listed as a GGDEF domain protein, actually lacks this domain, and thus we have not included it here. Finally, several proteins contain either incomplete domains or domains with degenerate motifs, and thus we have assigned those proteins to categories different from those listed on the website.

Mutants defective for c-di-GMP-related genes exhibit normal growth. To begin to understand the role of c-di-GMP in the physiology of *V. fischeri* strain ES114, we generated deletion mutants of the 50 c-di-GMP-related genes, regardless of whether they were predicted to encode catalytically active enzymes. In addition, we also generated double and/or triple deletions of genes contained within the putative operons, *VF_A0056-57*, *VF_A0342-343-344*, and *VF_A0475-476*, that consist of multiple DGC/PDE genes. We selected for gene replacement mutants using one of several different antibiotic resistance cassettes and then resolved the cassettes using Flp recombinase acting on FRT sequences flanking each resistance gene as described previously (26). A few of these single mutants have been reported separately (*lapD* [*VF_A1166*] and *pdeV* [*VF_A1014*] [34], *VF_1200* [37], and *casA* [*VF_1639*] [25]), and, as noted in the introduction, a few other genes have been characterized previously, including *mifA*, *mifB*, and *binA* (24, 38). Of the 55 mutants generated (including combinations), all exhibited normal growth characteristics in a rich medium (Fig. S3). Together, these data suggest that these proteins function to regulate cellular processes other than normal growth and metabolism under these conditions. In subsequent experiments, we assess the impact of these mutations on motility using the soft agar assay, which relies on not only motility but also growth (and chemotaxis). These growth experiments indicate that any motility defect we discover is unlikely to be due to a growth defect.

Six c-di-GMP-related proteins contribute to migration in magnesium-supplemented medium. We assessed the consequences of these mutations on bacterial motility by inoculating the mutants onto a tryptone-based soft agar medium supplemented with magnesium (TBS-Mg), which is known to promote *V. fischeri* motility (23). We measured the area of the migrating cells after a specific incubation period (4.5 h) and normalized the migration area to that of the wild-type strain on the same plates. Under these TBS-Mg conditions, only six mutants exhibited notable migration differences: two DGCs, three PDEs, and one dual DGC/PDE. The remainder of the mutants (including mutants defective for multiple genes within putative operons) migrated similarly to the wild-type strain (no deviation from wild-type migration greater than 15%), potentially because magnesium is a powerful motility stimulant (23) (Fig. 1 and Fig. S4).

Given that DGC-produced c-di-GMP inhibits motility, we expected that DGC mutants would exhibit increased motility. Of the DGC mutants, however, only the *mifB* mutant (*VF_A0959*) consistently exhibited increased migration, and it was only modestly increased relative to that of the wild-type (WT) strain (Fig. 1A). Of note, and as previously reported, both the *mifA* and *mifB* mutants lacked the robust center spot observed for wild-type strain ES114 (24) (Fig. 1C). The underlying signal transduction pathway(s) responsible for the formation of this center spot, a densely populated region of poorly swimming cells, remains unknown. We observed a similar phenomenon for the *VF_1200* mutant (Fig. 1C), which migrated about 10% more than the wild-type strain (Fig. S4), but not for any other mutant. These data suggest that the center spot can be attributed to the activities of these three proteins; loss of any one is sufficient to eliminate this phenotype, presumably by rendering the culture more uniformly motile under these conditions.

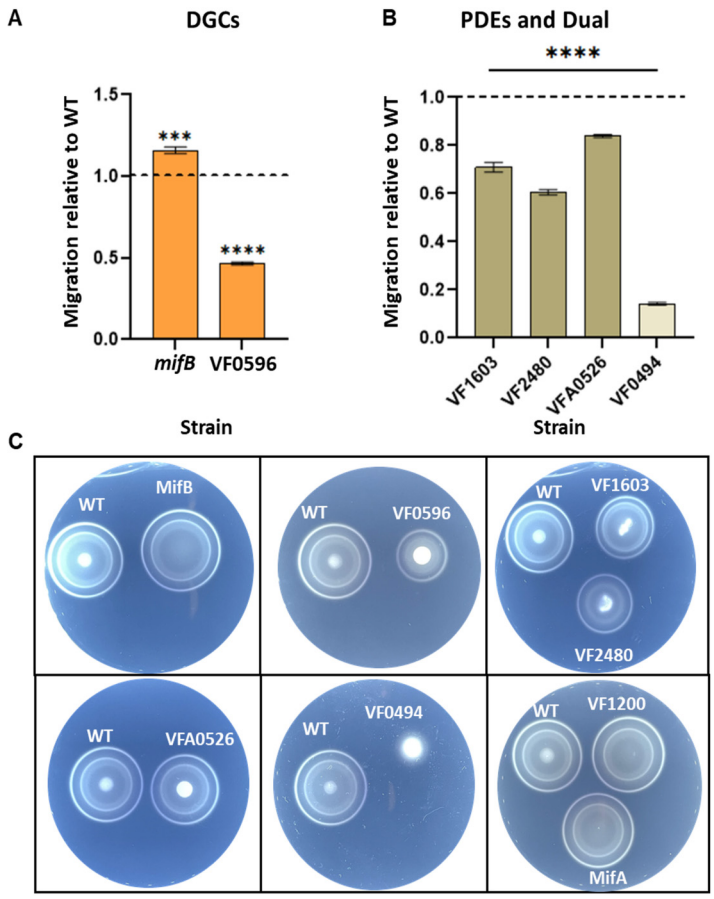

FIG 1 Migration of mutant strains on TBS-Mg. Migration of strains with significant changes relative to that of wild-type strain ES114 on TBS-Mg soft agar plates. (A and B) Graphs of the ratio of mutant migration relative to that of ES114. (A) DGCs. (B) PDEs and dual function. (C) Representative pictures of mutants with significant changes in migration and/or patterns relative to ES114, following growth on TBS-Mg. Pictures taken after 4.5 h. WT, wild-type strain ES114; the VF/VFA number indicates the gene that is deleted in the mutant. Error bars represent standard deviation. Data from a representative experiment performed with three technical triplicates are shown. The migration of each mutant was compared to the average migration of the wild-type strain present on the same soft agar plates and analyzed using an unpaired *t* test. ****, $P < 0.0001$; ***, $P \leq 0.001$.

The other DGC mutant exhibited a substantial decrease in migration, Δ*VF_0596* (Fig. 1A and Fig. S4A). Although a decrease in migration is not consistent with the predicted function of VF_0596, a similar phenomenon was reported for its *V. cholerae* homolog, CdgG (30); the two proteins exhibit 41% amino acid identity and 65% similarity (Table 5) across the length of the proteins, with both containing a C-terminal GGDEF domain. It will be of interest in the future to determine if these unusual regulators share other characteristics and/or regulons. At the current time, it is unclear why loss of VF_0596 would be detrimental for migration, but a few other DGC mutants also exhibited modestly decreased migration (less than 15% deviation from the wild-type migration) (Fig. S4B).

We expected PDE mutants to exhibit decreased migration due to increases in c-di-GMP levels, and indeed, this was the case. Mutants lacking the putative PDEs VF_1603, VF_2480, or VF_A0526 exhibited migration defects, with the Δ*VF_2480* mutant defect being the most severe of these (Fig. 1B and C). Of note, a single predicted dual-function protein, VF_0494, was critical for migration; the observed defect of the VF_0494 mutant was the strongest of any of the 50 mutants tested (Fig. 1B and C).

Thirteen genes are involved in controlling migration on TBS medium. Given that relatively few mutants exhibited phenotypes on TBS-Mg, we wondered if additional phenotypes would be observed if the strains were inoculated on TBS soft agar

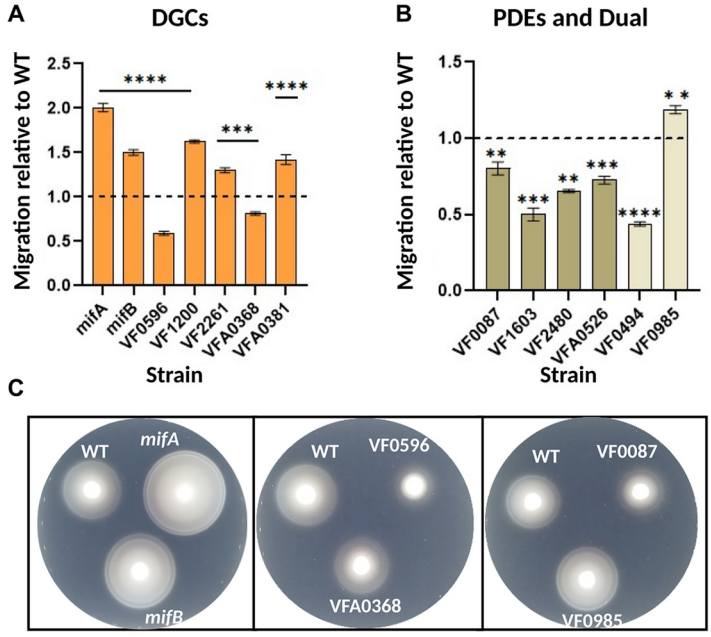

FIG 2 Migration of mutant strains on TBS. Migration of strains with significant changes relative to that of wild-type strain ES114 on TBS soft agar plates. (A and B) Graphs of the ratio of mutant migration relative to that of ES114. (A) DGCs. (B) PDEs and dual function. (C) Representative pictures of mutants with significant changes in migration relative to ES114, following growth on TBS. Pictures taken after 6.5 h. WT, wild-type strain ES114; the VF/VFA number indicates the gene that is deleted in the mutant. Error bars represent standard deviation. Data from a representative experiment performed with three technical triplicates are shown. The migration of each mutant was compared to the average migration of the wild-type strain present on the same soft agar plates and analyzed using an unpaired *t* test. ****, $P < 0.0001$; ***, $P \leq 0.001$; **, $P \leq 0.01$.

medium lacking Mg. ES114 migrates considerably more slowly through this medium, and thus we increased the incubation time to 6 to 7 h. We found that, indeed, 13 of the set of 55 strains (including operon mutants) exhibited altered migration under these conditions, compared to 6 in TBS-Mg (Fig. 2 and Fig. S5). The phenotypes of DGC mutants lacking VF_0596 or MifB (VF_A0959) were similar on the two media, albeit with a larger difference on TBS for the latter (Fig. 2A). Moreover, the TBS conditions revealed altered migration phenotypes for five additional DGC mutants; those lacking MifA (VF_0989) exhibited a striking increase, while those lacking VF_1200, VF_2261, or VF_A0381 had more modest but significantly increased migration (Fig. 2A). Additionally, the Δ*VF_A0368* mutant exhibited modestly decreased migration (Fig. 2A). For the PDE mutants, the decreased migration seen for strains lacking VF_1603, VF_2480, or VF_A0526 on TBS-Mg also occurred on TBS. A small but significant decrease in migration was observed for PDE mutant Δ*VF_0087* (Fig. 2B). Finally, the dual DGC/PDE mutant lacking VF_0494 retained a migration defect (albeit slightly less severe), while a mutant lacking VF_0985 consistently exhibited a small but significant increase in migration (Fig. 2C). None of the other mutants, including those defective for multiple genes within putative operons, exhibited a consistent defect in migration (greater or less than 15% of wild-type migration) (Fig. S5).

Sixteen c-di-GMP-related proteins influence migration in calcium-supplemented medium. Finally, we assessed the consequences of these mutations on the ability of *V. fischeri* to migrate through TBS soft agar supplemented with 10 mM calcium chloride (TBS-Ca). Supplementation with 10 mM calcium promotes migration relative to unsupplemented TBS medium (23) but to a lesser extent than when magnesium is added. As a result, we evaluated migration following incubation on soft agar plates for approximately 5.5 h. Like TBS, the TBS-Ca condition also revealed a large number of mutants (16) to be defective (Fig. 3 and Fig. S6), but there was only a partial overlap between the two conditions.

Five of the DGC mutants exhibited the same relative migration pattern on TBS-Ca as they did on TBS (mutants deleted for *VF_0596*, *mifA* [*VF_0989*], *VF_1200*, *VF_A0381*,

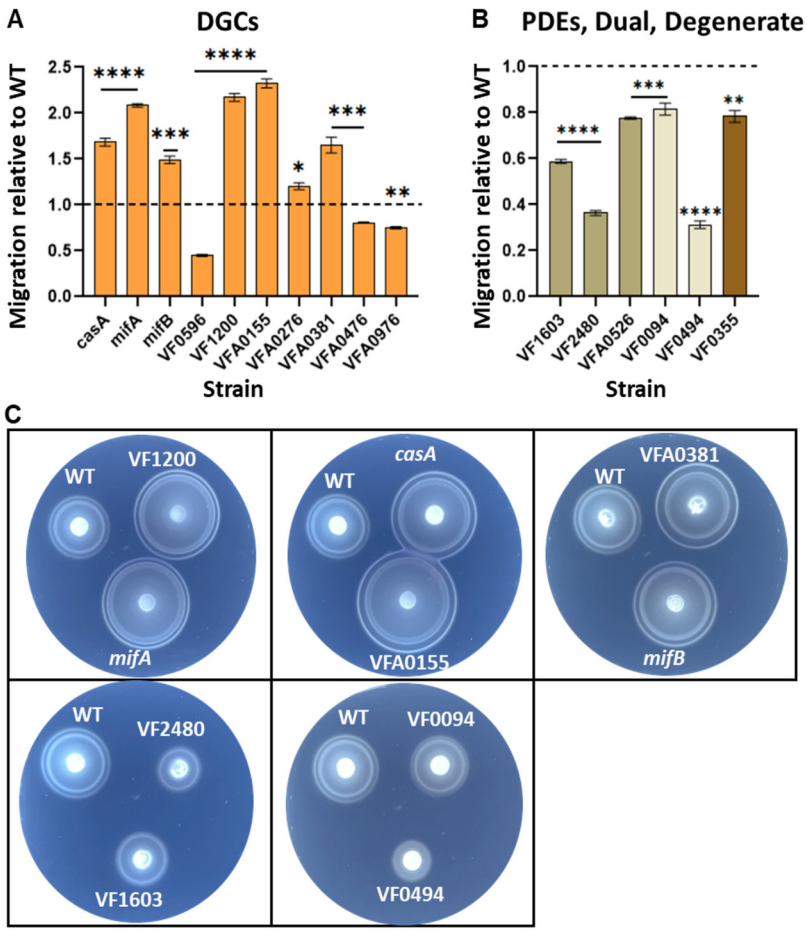

FIG 3 Migration of mutant strains on TBS-Ca. Migration of strains with significant changes relative to that of wild-type strain ES114 on TBS-Ca soft agar plates. (A and B) Graphs of the ratio of mutant migration relative to that of ES114. (A) DGCs. (B) PDEs, dual function, and degenerate. (C) Representative pictures of mutants with significant changes in migration relative to ES114, following growth on TBS-Ca. Pictures taken after 5.5 h. WT, wild-type strain ES114; the VF/VFA number indicates the gene that is deleted in the mutant. Error bars represent standard deviation. Data from a representative experiment performed with three technical triplicates are shown. The migration of each mutant was compared to the average migration of the wild-type strain present on the same soft agar plates and analyzed using an unpaired *t* test. ****, $P < 0.0001$; ***, $P \leq 0.001$; **, $P \leq 0.01$; *, $P \leq 0.05$.

or *mifB* [*VF_A0959*]) (Fig. 3A). Two DGC mutants with phenotypes on TBS failed to exhibit phenotypes on TBS-Ca (defective for *VF_2261* or *VF_A0368*). Of note, the TBS-Ca condition uncovered phenotypes for five additional DGCs not observed on TBS: *casA* (*VF_1639*; a phenotype reported by reference 25), *VF_A0155*, *VF_A0276*, *VF_A0476*, and *VF_A0976* (Fig. 3A).

For the PDE mutants (Fig. 3B), the behaviors of the *VF_2480*, *VF_1603*, and *VF_A0526* mutants on TBS-Ca were similar to those observed on TBS, although the relative severity of the defect of the former two mutant strains was different: the *VF_2480* mutant exhibited a greater migration defect on TBS-Ca (and on TBS-Mg) than the *VF_1603* mutant, whereas the migration defects of the two mutants on TBS were opposite, with the *VF_1603* mutant migrating worse than the *VF_2480* mutant.

As with the other conditions, a mutant defective for the putative dual regulator VF_0494 migrated poorly on TBS-Ca; this mutant was not only consistently defective across the media types, but it also exhibited the most severe defects of all the strains under all conditions. The small increase in migration observed on TBS for putative dual regulator mutant Δ*VF_0985* was lost on TBS-Ca, while small defects for mutants of VF_0094 (a putative dual regulator) and VF_0355 (a putative nonenzymatic protein)

were observed (Fig. 3B). None of the other mutants exhibited consistent, significant changes in migration on TBS-Ca relative to that of the wild-type control (Fig. S6). Altogether, TBS-Ca conditions revealed phenotypes for 16 mutants, similar in number to but not fully overlapping that seen with the TBS conditions; both of these conditions were superior to TBS-Mg, which uncovered only 6 mutants with phenotypes. Thus, the use of different medium conditions provided valuable insights into gene function and permitted us to uncover more subtle—or potentially condition-specific—phenotypes.

Inhibition of motility at high calcium occurs primarily via CasA. Because the calcium conditions provided the greatest insight by identifying the greatest number of mutants with phenotypes, we extended our experiments for a subset of strains by increasing the amount of calcium in the motility agar. Relative to its absence, addition of 10 mM calcium increases migration of ES114, whereas larger amounts, such as 40 mM calcium, impair it (23). We recently reported that a mutant lacking the DGC CasA (*VF_1639*) migrates robustly through soft agar containing calcium at levels up to 100 mM and produces c-di-GMP in response to calcium in a heterologous microbe (*Escherichia coli*) (25). While the *casA* mutant was one of the nine DGC and dual mutants that exhibited increased abilities to migrate through TBS-Ca (10 mM) (Fig. 3), it did not exhibit the greatest increase. Rather, a strain deleted for *VF_A0155* exhibited the greatest increase, with the Δ*mifA* and Δ*VF_1200* mutants both migrating more than the Δ*casA* mutant. Thus, we wondered whether these mutants would also migrate robustly at increased concentrations of Ca. We tested a subset of these mutants (*mifA* [*VF_0989*], *VF_1200*, *casA* [*VF_1639*], *VF_A0155*, *VF_A0381*, and *mifB* [*VF_A0959*]) on media containing larger amounts of calcium. Despite the substantial migration observed for the *VF_A0155* mutant on TBS-Ca (10 mM), neither this nor the other tested mutants phenocopied the *casA* mutant for migration on larger amounts of Ca (20, 30, or 40 mM) (Fig. 4). These data provide additional support for the key role of CasA in responding to high levels of calcium (25) and suggest that the 10 mM condition may provide distinct information relative to higher calcium levels.

c-di-GMP levels influenced by Mg and Ca. Using a c-di-GMP riboswitch biosensor in which the gene for red fluorescent protein (RFP) is positively controlled by c-di-GMP (39, 40), we previously reported that increasing amounts of calcium caused increasing levels of c-di-GMP in a medium distinct from that used here (25). Because ES114 migrates at different rates under the three conditions in this study, TBS, TBS-Mg, and TBS-Ca (23), we wondered whether these conditions resulted in altered levels of c-di-GMP. Levels of RFP, the output of the c-di-GMP biosensor, were modestly but significantly diminished by addition of low levels of Ca (10 mM) relative to unsupplemented TBS, consistent with the slightly increased ability of ES114 to migrate through TBS-Ca (10 mM) relative to TBS (23) (Fig. 5A). In contrast, addition of higher levels of Ca (20 and 30 mM) to TBS increased levels of the biosensor, as seen previously using different medium conditions (25). These data provide an explanation for the differential migration under different amounts of Ca (23).

We next probed the impact of the addition of Mg. The 35 mM concentration of Mg has been historically used in *V. fischeri* motility experiments because this amount approximates that found in seawater and is thus biologically relevant for this marine microbe. We found that addition of 35 mM Mg resulted in substantially decreased levels of RFP, whereas addition of a smaller amount (1 mM Mg) trended lower but did not reach the level of significance (Fig. 5B). These data thus add Mg to the list of signals that control c-di-GMP levels in *V. fischeri* and provide an explanation for the ability of Mg to robustly promote *V. fischeri* flagellation and motility (23).

Ca-induced motility defect can be suppressed by *flrA* point mutation. In *V. cholerae*, the master flagellar regulator, FlrA, is subject to control by c-di-GMP (41). FlrA variants with substitutions in the c-di-GMP-binding residues R135 (R135H) and R176 (R176H) exhibit decreased binding to c-di-GMP and thus permit increased motility for specific strains grown under conditions of high c-di-GMP (41). *V. fischeri* FlrA is similarly required for motility (20, 26), and the R135 and R176 residues are conserved, but the role of c-di-GMP in controlling its activity has not been reported. Thus, we generated strains that expressed wild-type FlrA, FlrA-R135H, or FlrA-R176H from a nonnative location in

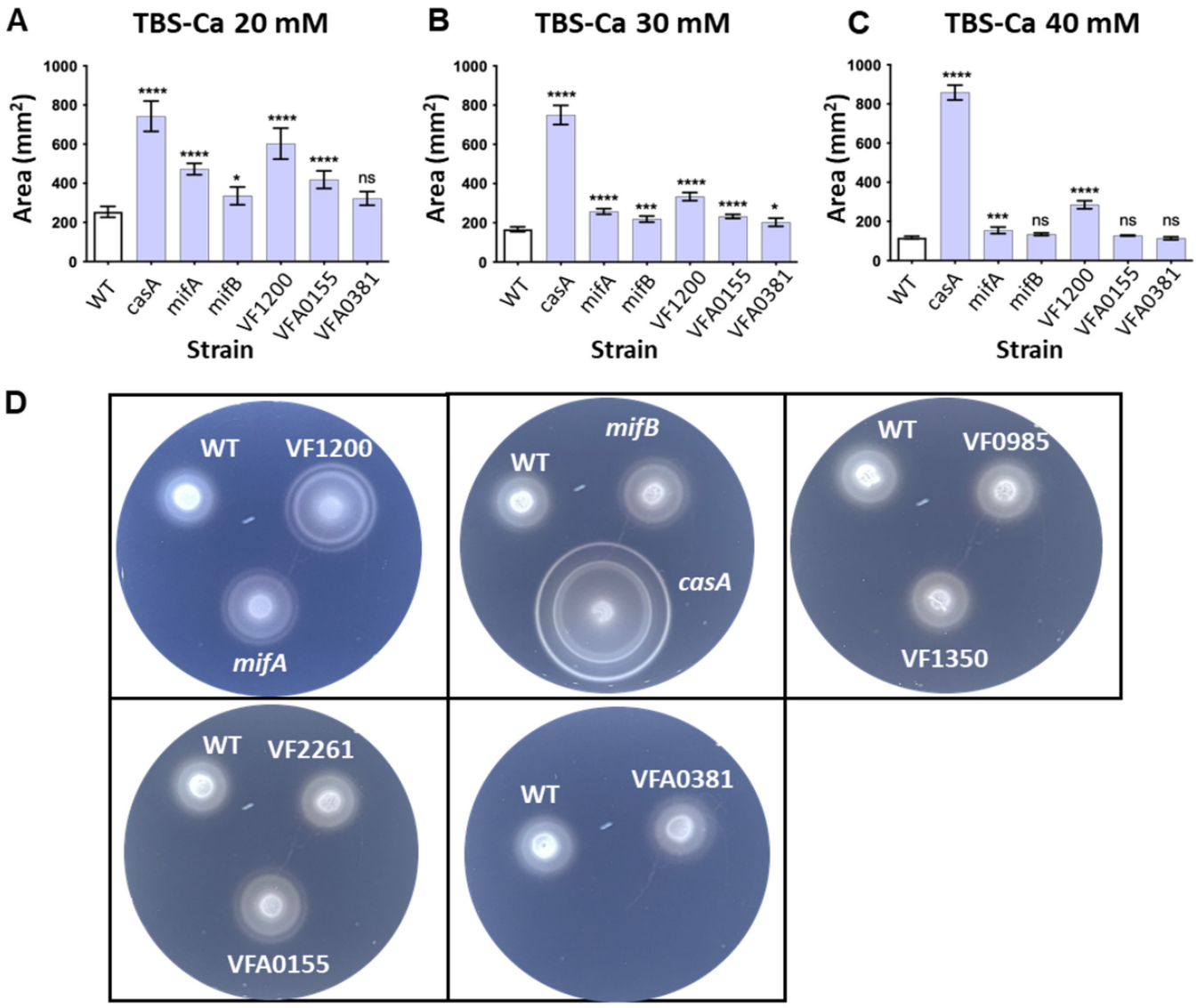

FIG 4 Migration of selected mutant strains on TBS plates containing different concentrations of Ca. Areas of migration for mutants lacking the following proteins were assessed on TBS containing (A) 20 mM Ca, (B) 30 mM Ca, or (C) 40 mM Ca. Migration on TBS with 20 or 30 mM Ca was assessed at 5.5 h, while migration on TBS with 40 mM was assessed at 6 h. (D) Representative pictures of strains on TBS-Ca (30 mM) at 5.5 h. WT, wild-type strain ES114; the VF/VFA number indicates the gene that is deleted in the mutant. Error bars represent standard deviation. A representative experiment, one of at least two performed, is shown and incorporates three technical replicates. Statistical analyses were done using one-way ANOVA and Dunnett's test for multiple comparison. ****, $P < 0.0001$; ***, $P \leq 0.001$; *, $P \leq 0.05$; ns, not significant.

the chromosome and evaluated their ability to complement the nonmotile *flrA* mutant. Indeed, expression of each of the three versions of FlrA restored wild-type migration to the *flrA* mutant on TBS-Mg (Fig. 6A). Moreover, when the strains were inoculated onto TBS-Ca (10 mM) soft agar, the two point-mutant derivatives were far superior in their ability to promote migration relative to the wild-type-complemented strain (Fig. 6B). These data indicate that Ca, presumably due to induction of higher levels of c-di-GMP, inhibits migration via an impact on FlrA activity and that each of the point mutations rendered *V. fischeri* FlrA "blind" to c-di-GMP. At 20 mM Ca, while the ability of these variants to promote migration relative to wild-type FlrA remained superior, the overall migration of the strains was reduced compared to the 10 mM Ca condition (Fig. 6B and C), indicating that there are likely other processes being affected by the high levels of c-di-GMP. For example, growth of *V. fischeri* is reduced by high levels of Ca (25).

In *V. cholerae*, observing the effect of these mutations on bacterial motility requires the additional disruption of genes involved in polysaccharide biosynthesis (*vps*) (41).

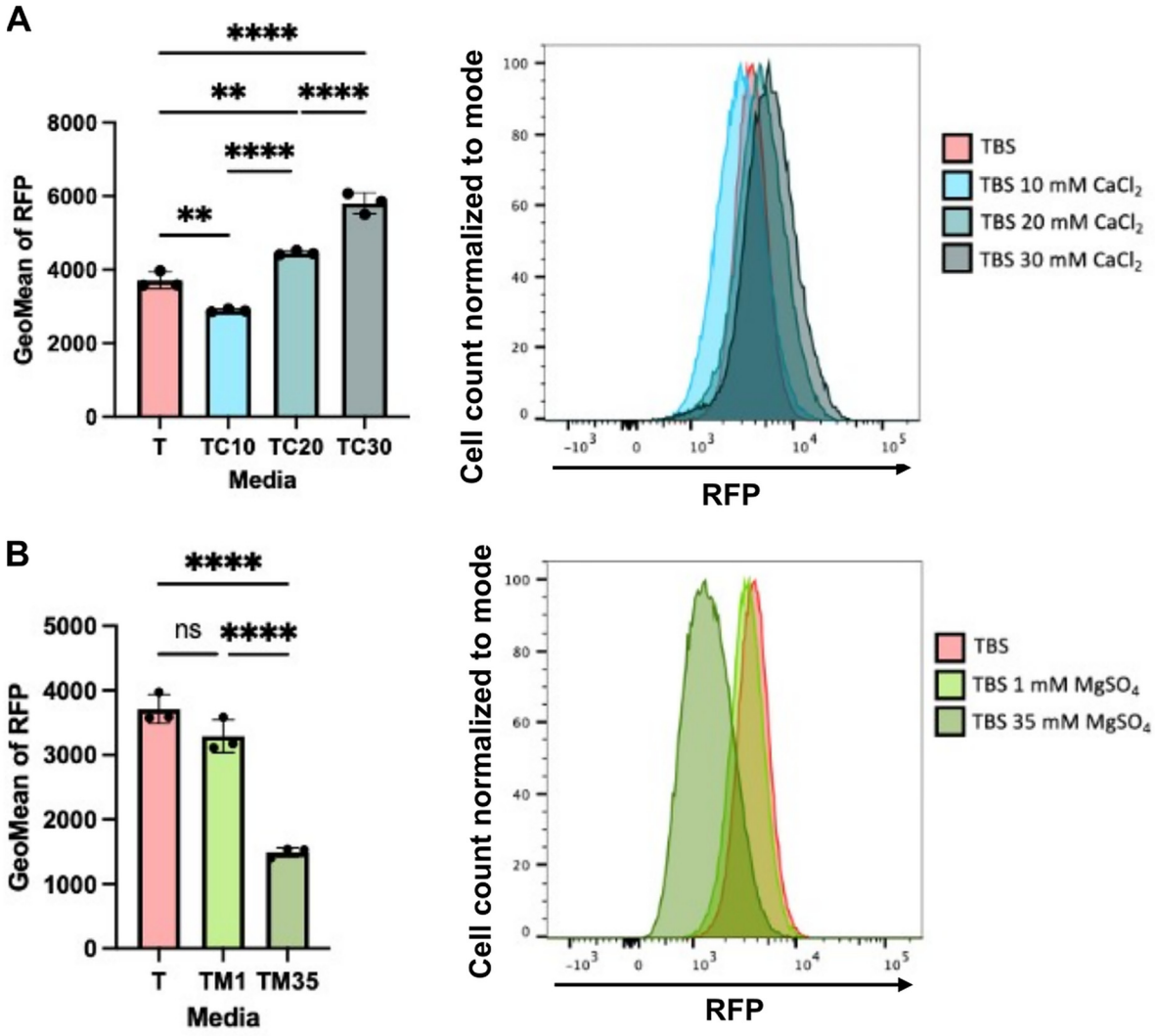

FIG 5 Effect of calcium and magnesium on c-di-GMP levels. RFP levels (reflective of c-di-GMP levels) in cells carrying the c-di-GMP biosensor pFY4535 were measured by flow cytometry following growth in TBS supplemented with (A) 10, 20, or 30 mM $CaCl_2$ (TC10, TC20, and TC30, respectively) or (B) 1 or 35 mM $MgSO_4$ (TM1 and TM35, respectively) and compared to unsupplemented TBS (T) and each other. Cells were gated on double positive AmCyan/RFP, and the number of cells was normalized to mode. Geometric mean (GeoMean) of the resulting curves was used for quantification. For panels A and B, each of the dots represents biological replicates and the error bars represent standard deviation; the TBS data are the same in the two panels. Statistics were performed by one-way ANOVA (**, $P < 0.005$; ****, $P < 0.0001$).

However, disruption of additional genes was not necessary to observe an effect in *V. fischeri*. Rather, a simple manipulation of the growth media to induce higher levels of c-di-GMP was sufficient to observe an effect of these point mutations on *V. fischeri* migration.

Double and triple mutants exhibit more severe motility defects on TBS-Mg. Finally, we pursued the construction of a limited number of strains with multiple mutations (other than the operon mutants described above) in an effort to generate strains with enhanced phenotypes. We focused our efforts on the investigation of three genes, *VF_0494*, *VF_1603*, and *VF_2480*. The first was of interest because of the consistent and severe defect observed for the Δ*VF_0494* mutant across the different media. Similarly, mutants lacking either of the other two genes *VF_1603* and *VF_2480* exhibited consistent, albeit milder, migration defects as well. Because the proteins of these genes share 46% identity and 69% similarity (Table 5), we wondered if a double mutant would exhibit a greater defect in migration and found that it did (Fig. 7A and B).

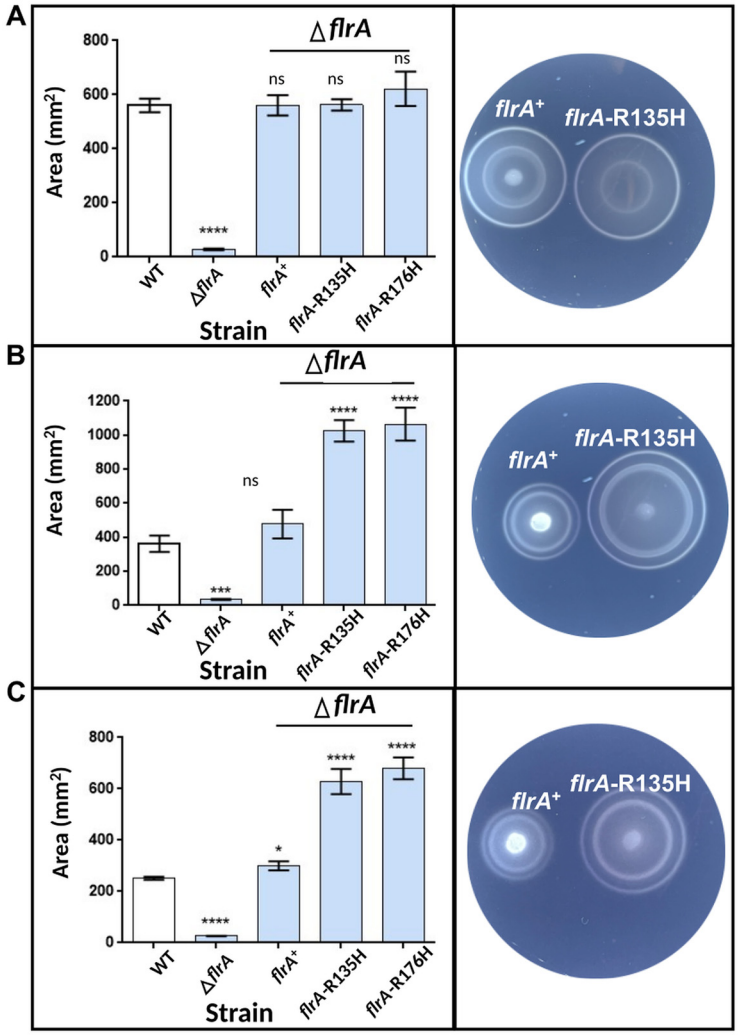

FIG 6 Migration of strains containing "c-di-GMP-blind" alleles of *flrA*. Left: areas of migration of strains containing "c-di-GMP-blind" alleles of *flrA* were assessed on TBS soft agar containing (A) 35 mM Mg, (B) 10 mM Ca, or (C) 20 mM Ca. Right: Corresponding representative images for Δ*flrA flrA*$^+$ and Δ*flrA flrA*-R135H strains. TBS-Mg plates were assessed at 4.5 h, while TBS-Ca (10 mM and 20 mM) plates were assessed at 5.5 h. Error bars represent standard deviation. A representative experiment, one of at least two performed, is shown and incorporates three technical replicates. Statistical analyses were done using one-way ANOVA and Dunnett's test for multiple comparison. ****, $P < 0.0001$; *, $P \leq 0.05$; ns, not significant.

Furthermore, whereas derivatives in which the Δ*VF_0494* mutation was combined with either Δ*VF_1603* or Δ*VF_2480* retained their ability to migrate, albeit poorly, a combination mutant deleted for all three genes failed to migrate within the 5-h time course (Fig. 7A and B), although migration did occur following prolonged incubation.

To determine if the observed defects in migration could be attributed to high levels of c-di-GMP, we evaluated the ability of a PDE (VF_0087), introduced on plasmid pKV302, to restore wild-type migration; this PDE has been effective in promoting *V. fischeri* migration in other contexts (37). Indeed, pKV302 restored some migration of the triple mutant relative to that of the vector control; however, it did not permit wild-type levels of migration (Fig. 7C). It is possible that this PDE could not sufficiently remove the c-di-GMP to fully permit migration, or else that there are other consequences due to the loss of one or more of these proteins. To further understand the consequences of the losses of VF_0494, VF_1603, and VF_2480, we introduced the "c-di-GMP-blind" *flrA-R135H* allele into the single Δ*VF_0494* mutant as well as the double *VF_1603/VF_2480*

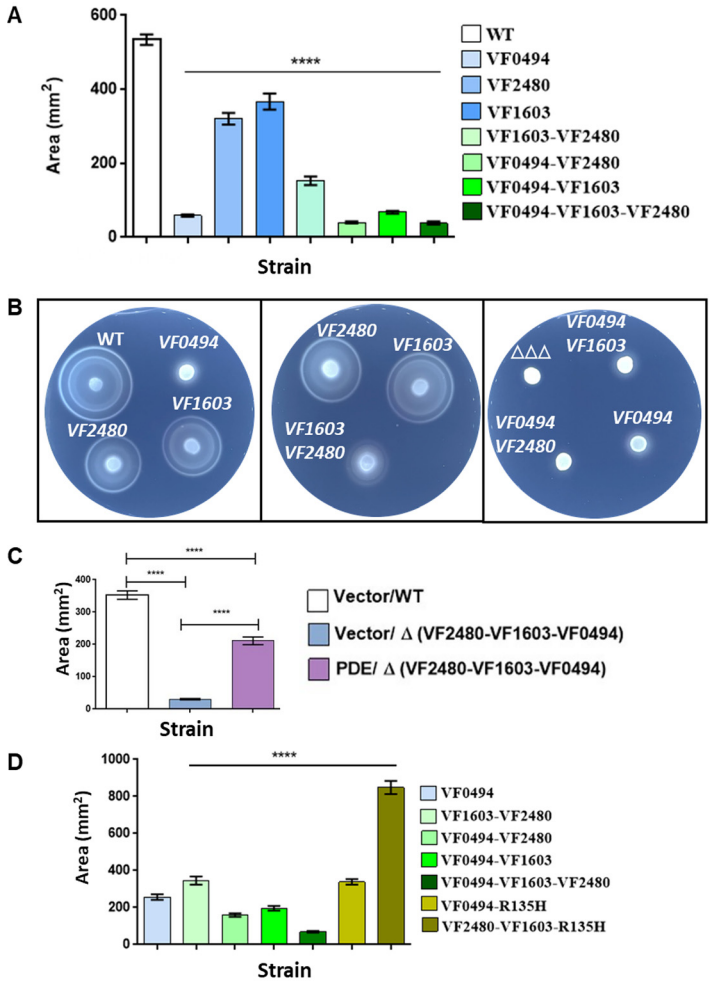

FIG 7 Migration of strains containing double and triple mutations. Areas of migration were assessed on TBS soft agar containing 35 mM Mg (and, for panel C, chloramphenicol). (A and B) Migration was assessed for strains containing double and triple deletions of *VF_0494*, *VF_1603*, and *VF_2480* at 4.5 h. (C) Migration of the triple mutant (Δ*VF_2480* Δ*VF_1603* Δ*VF_0494*) containing either the PDE overexpression plasmid pKV302 or its vector control pKV69 was assessed at 4.5 h; (D) Migration of the single, double, and triple mutants containing or lacking *flrA*-R135H as indicated was assessed after 6 h. WT, wild-type strain ES114; the VF/VFA number indicates the gene that is deleted in the mutant; the triple (Δ*VF_2480* Δ*VF_1603* Δ*VF_*0494) is also shown as ΔΔΔ. Error bars represent standard deviation. A representative experiment, one of at least two performed, is shown and incorporates three technical replicates. Statistical analyses were done using one-way ANOVA and Dunnett's test for multiple comparison. For panel C, one-way ANOVA and Sidak's multiple-comparison test were used. For panel D, the comparison was made to the Δ*VF_0494* mutant. ****, $P < 0.001$.

mutant. Migration of the double mutant was robustly restored (Fig. 7D), suggesting that these two genes affect c-di-GMP levels that in turn control FlrA activity. However, migration was only weakly restored to the Δ*VF_0494* mutant by the presence of the *flrA-R135H*; this is similar to our observations that this allele was not sufficient to restore motility in high calcium and suggests that either (i) the c-di-GMP produced by the Δ*VF_0494* mutant acts at levels other than FlrA activity to control motility or (ii) VF_0494 has a distinct function in motility besides controlling c-di-GMP levels. Future work will distinguish between these possibilities.

Overall conclusions. This work identified roles in motility for a subset of 50 *V. fischeri* genes with putative GGDEF, EAL, and HD-GYP domains. Of note, the use of media supplemented with or lacking added Mg or Ca provided additional insights into the requirements for specific genes in this phenotype (Fig. 8). These cations influence the levels of c-di-GMP corresponding to their impact on *V. fischeri*'s ability to migrate through soft agar; in particular, we report here the dramatic effect that Mg supplementation exerts

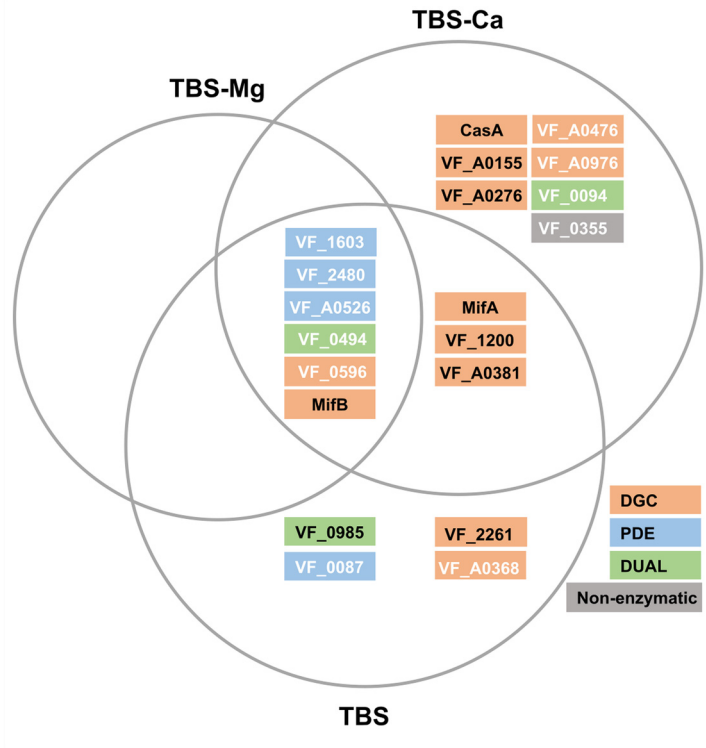

FIG 8 Model of genes required for *V. fischeri* motility under different conditions. Venn diagram depicting the three conditions under which bacterial migration was assessed, TBS-Mg, TBS, and TBS-Ca, and the genes whose loss affects motility under those conditions. The colors of the boxes represent the grouping of the indicated gene: orange, DGC; blue, PDE; green, dual; and gray, nonenzymatic. The color of the text represents the direction of the impact of mutation: up, black; down, white.

over c-di-GMP levels, consistent with its known ability to promote motility of *V. fischeri* (23). We found that the inhibition of motility caused by the addition of Ca can be suppressed by expression of either of two "c-di-GMP-blind" alleles of the master regulator *flrA*. Finally, we identified three genes (*VF_0494*, *VF_1603*, and *VF_2480*) that play central roles (potentially somewhat redundant, in the case of *VF_1603* and *VF_2480*) in controlling the ability of *V. fischeri* to migrate through soft agar.

Liu et al. performed similar work in *V. cholerae*, with the disruption of 52 GGDEF- and/or EAL-domain-encoding genes (28). That study reported that only 7 of the 52 mutants exhibited altered motility, with three decreased (*cdgJ*, *rocS*, and *cdgG* mutants) and four increased (*cdgH*, *cdgK*, *cdgL*, and *cdgD* mutants) under the assay conditions, LB soft agar incubated at 30°C; this small number is similar to that which we observed on TBS-Mg conditions (six mutants). *V. fischeri* carries homologs for four of those seven genes. Indeed, mutants defective for the homologs of *V. cholerae cdgJ* (*VF_2480*), *rocS* (*VF_0494*), *cdgG* (*VF_0596*), and *cdgK* (*casA* [*VF_1639*]) behaved the same, with decreased or increased migration in soft agar (albeit for Δ*casA* only when calcium was present), suggesting a conservation of function across species. In *V. cholerae*, *cdgJ* exerted the greatest impact, while the effect of *rocS* disruption was milder, whereas the opposite was true for mutants of the *V. fischeri* homologs, with disruption of the *rocS* homolog *VF_0494* exerting the greatest impact on migration. Of note, although *V. cholerae* carries *cdgJ* and a *cdgJ*-like gene, *VC_1851*, homologous to *V. fischeri* genes *VF_2480* and *VF_1603*, respectively, a motility defect was not reported for a Δ*VC_1851* mutant. It will be of interest to see if a *V. cholerae* mutant defective for *cdgJ* and *VC_1851* correspondingly exhibits a greater defect in migration than the *cdgJ* single mutant.

This work focused on GGDEF, EAL, and HD-GYP domain-carrying proteins, so it did not incorporate the study of putative c-di-GMP-binding elements, such as PilZ domain

genes (12, 42), riboswitches (43), or the relatively newly identified MshEN domain found in the c-di-GMP-binding MshE (44, 45). *V. fischeri* carries four PilZ domain genes, at least one putative riboswitch, and MshE (VF_0362) (https://www.ncbi.nlm.nih.gov/Complete_Genomes/c-di-GMP.html) (2, 5, 12, 13). With the foundational work described here, the impact of these and other putative c-di-GMP-binding proteins and riboswitches can be analyzed more readily using mutants either with single or multiple DGC or PDE gene deletions or with the addition of specific amounts of Mg or Ca. Together, this work sheds light on the genes and conditions that influence c-di-GMP-mediated control over motility in *V. fischeri* and provides a foundation for (i) assessing roles of putative c-di-GMP-binding proteins, (ii) evaluating other c-di-GMP-dependent phenotypes in *V. fischeri*, (iii) uncovering potential redundancy, and (iv) deciphering signal transduction mechanisms.

MATERIALS AND METHODS

Bioinformatic analyses. Each of the 50 proteins previously identified as containing GGDEF and/or EAL or HY-GYP domains (see reference 16 and https://www.ncbi.nlm.nih.gov/Complete_Genomes/c-di-GMP.html) (2, 5, 12, 13) was submitted to BLASTP with the default settings (46). The graphical summary and corresponding alignments (47–49) were used to identify possible domains, both c-di-GMP-related (GGDEF, EAL, HD-GYP) domains and others found in the database. These putative domains (see Fig. S1 in the supplemental material) are largely the same as identified previously (16). Analysis of the presence of the GGDEF, EAL, HD-GYP, and I-site motifs were performed using the alignments and the known conserved amino acids. To determine the possible membrane-associated regions (Fig. S2), we submitted protein sequences to TMPred (50) or Protter (51). Finally, to evaluate the similarity between *V. fischeri* and *V. cholerae* proteins, *V. fischeri* sequences were submitted to BLASTP using *V. cholerae* O1 biovar El Tor strain N16961 (27) in the organism search set. The corresponding *V. cholerae* proteins were similarly submitted to BLASTP, selecting *V. fischeri* ES114 (14, 15) in the organism search set; the numbers listed in Table 5 were taken from the resulting alignments in this analysis.

Strains and media. *V. fischeri* strains were derived from ES114 (52) and are listed in Table S1. They were routinely cultured in LB-salt (LBS; 1% tryptone, 0.5% yeast extract, 2% sodium chloride, and 50 mM Tris [pH 7.5] [19]) liquid or solidified with agar to a final concentration of 1.5%, with some exceptions: LB (1% tryptone, 0.5% yeast extract, 1% sodium chloride) liquid or solidified with agar to a final concentration of 1.5% was used when certain antibiotics specified below were used. For motility experiments, TBS (1% tryptone, 2% sodium chloride) and TBS solidified with 0.25% agar alone or supplemented with 35 mM magnesium sulfate (Mg) or 10 mM calcium chloride (Ca) were used; other amounts of Mg and Ca were used in specific experiments as indicated. We note that the source of tryptone can affect this phenotype, and thus we consistently used Difco (Gibco) tryptone for all motility experiments. To promote consistency between experiments, the same volume (25 mL) was pipetted into each petri dish on the day prior to a given experiment. For genetic manipulation, cells were grown in TMM (100 mM Tris [pH 7.5], 300 mM NaCl, 0.1% ammonium chloride, 10 mM *N*-acetylglucosamine, 50 mM $MgSO_4$, 10 mM KCl, 10 mM $CaCl_2$, 0.0058% K_2HPO_4, 10 μM ferrous ammonium sulfate) as described below to generate competent cells. Antibiotics were added as needed to the following final concentrations: chloramphenicol (Cm), 1 μg mL^{-1}; erythromycin (Em), 2.5 μg mL^{-1}; gentamicin (Gm), 5 μg mL^{-1}; kanamycin (Kn), 100 μg mL^{-1} (*V. fischeri*) or 50 μg mL^{-1} (*E. coli*); spectinomycin (Sp), 200 μg mL^{-1}; tetracycline (Tc), 2.5 μg mL^{-1}; and trimethoprim (Tm), 2.5 μg mL^{-1}. LB was used instead of LBS with Sp or Gm supplementation.

E. coli strains were used for conjugation to introduce plasmids into *V. fischeri*. Plasmids used are listed in Table S2 and include conjugal plasmid pEVS104 (53), Flp recombinase plasmid pKV496 (26), or TfoX-producing plasmids plostfoX (54), plostfoX-Kan (55), or pJJC4 (56). *E. coli* strains were cultured in LB. Antibiotics were added as needed to the following final concentrations: Cm, 12.5 μg mL^{-1}; Kn, 50 μg mL^{-1}. Thymidine was added as needed to a final concentration of 0.3 mM for use with *E. coli* thymidine auxotrophic strains.

Construction of mutants. Strains were constructed as described previously (26, 57) using plasmids and primers listed in Tables S2 and S3, respectively. Briefly, sequences (about 500 bp) upstream and downstream of the gene of interest were amplified using EMD Millipore KOD polymerase in a PCR with primers containing linker sequences. A third PCR product, containing an antibiotic resistance cassette, was amplified from plasmid templates (Table S2) with primers 2089 and 2090 (Table S3). The three PCR products were fused together using a splicing by overlap extension (SOE) technique (58). The composite DNA fragments were introduced by transformation into ES114 containing a *tfoX*-overexpression plasmid. Competent cells were generated and transformations were carried out as described previously (57), with selection for the antibiotic resistance cassette. The deletion of interest was confirmed using *Taq* polymerase in a PCR with the outside primers. In some cases, mutants were first generated in an intermediate strain, such as a *tfoX*-carrying Δ*qrr1* mutant (56), and genomic DNA from the resulting strain was used in a subsequent transformation to introduce the gene replacement mutation into ES114. Similarly, strains carrying more than one deletion were generated by introducing genomic DNA generated from a marked (with an antibiotic resistance cassette) mutant of interest into a *tfoX*-overexpressing recipient strain carrying one or more other mutations. Antibiotic resistance markers were flanked by FRT sequences and were resolved using Flp recombinase expressed from pKV496, as described previously (26, 57), to reduce the concern of a polar effect due to the insertion and to readily permit the construction of strains with multiple deletions. This approach leaves a small scar at the deletion site.

Construction of *flrA* alleles. PCR was used to introduce point mutations into the *flrA* gene as follows. To generate P*flrA-flrA*-R135H, strain KV8290 (26), which carries an *flrA* deletion (and an FRT scar) and an *flrA* complementation cassette in the intergenic region between *yeiR* and *glmS* (*VF_2380-VF_2372*), was used as a template in two separate reactions, with primer pairs 2290 & 2256 and 2255 & 1487. The resulting PCR products were combined and used in a PCR SOE reaction to generate full-length *flrA* with the point mutation, which was subsequently introduced by transformation into a *tfoX*-overexpressing derivative of KV8232 (26). A similar approach was used to generate P*flrA-flrA*-R176H, using primer pairs 2290 & 2258 and 2257 & 1487. When strains carrying the complementation constructs were obtained, genomic DNA was isolated and used to transform a *tfoX*-overexpressing derivative of the Δ*flrA* strain KV8148 or similarly introduced into the strains with mutations in *VF_0494*, *VF_1603*, and/or *VF_2480*.

Evaluation of growth. Growth of all strains in the present study was assessed in 96-well plates by the Molecular Devices SpectraMax iD3 multi-mode microplate reader. Kinetic absorbance mode was used to chart strains over 16 h, with reads every 14.5 min and medium shaking for 10 s between reads. Absorbance was measured at a wavelength of 600 nm. The data were then plotted using Excel.

Assessment of motility. Strains were grown overnight (14 to 16 h) with shaking in TBS medium at 28°C and then subcultured into fresh TBS and incubated with shaking at 28°C for ~3 h. The growth of the strains was estimated by measuring the optical density at 600 nm (OD_{600}). The OD_{600} was normalized to 0.2 using TBS as a diluent. An aliquot (10 μL) of each strain was spotted in triplicate onto different petri plates containing TBS soft agar (0.25% agar) with or without supplementation (generally with 35 mM $MgSO_4$ or 10 mM $CaCl_2$ but with other concentrations as indicated; technical replicates). Following 4 to 7 h of incubation at 28°C, all plates were photographed. For all motility experiments, each strain was assessed as described above at least two times (two biological replicates each with three technical replicates); those that are shown in Fig. 1 to 3 were performed at least three times or more. For the experiments shown in Fig. 1 to 3 and the corresponding supplemental data Fig. S4 to S6, subsets of the strains were assessed on different days; as a result, each mutant strain was compared to the average migration of the wild-type strain present on the same plates. For the other motility experiments, a representative experiment with three technical replicates performed with all the indicated strains on the same day is shown; at least two such experiments were performed.

Motility spot analysis. Images were analyzed using Fiji (ImageJ) software. Spot area was measured using the oval selection tool to surround spots at their outermost growth (at the edge of rings when present, or visible growth when rings were less/not apparent); in some cases, the outermost growth was faint. The consistent scale used was 15.4737 pixels/mm, and this was set from the diameter of one spot measured by hand. All images analyzed were taken from the same distance, with 33.3% zoom. For the evaluation of the 50 single mutants and 5 operon mutants, the migration of each mutant was normalized to the migration of the wild-type strain ES114 present on the same plate by dividing mutant migration area by average wild-type migration area. No contrast adjustments or other digital manipulations were used to process images.

c-di-GMP biosensor measurements. Strains were grown with shaking overnight in TBS at 28°C and subcultured the following morning in various conditions (TBS, TBS with 10, 20, or 30 mM $CaCl_2$, or TBS with 1 or 35 mM $MgSO_4$) for 5 h. The biosensor was selected using gentamicin throughout growth. Ten microliters of the subculture was added to 1 mL phosphate-buffered saline (PBS). Samples were then analyzed by flow cytometry on the BD Sciences LSRFortessa system. A threshold of 500 was set for forward scatter (FSC) and side scatter (SSC) in log scale. AmCyan and RFP were visualized using two channels, AmCyan and phycoerythrin (PE)-Texas Red, respectively. Data were compiled using BD Sciences FlowJo version 10.8 and GraphPad Prism version 9.1.2. FSC and SSC gating determined live cells. Double positive AmCyan and RFP cells were further analyzed by creating histograms for RFP. The resulting curves were quantified by the geometric mean fluorescence intensity (MFI) for comparison after normalization to mode. Statistical analyses were performed using one-way analysis of variance (ANOVA).

Statistical measurements. Statistical analyses for motility experiments were done in GraphPad Prism 9. Assessing the large number of strains and conditions required many experiments over numerous days. To normalize the large number of results derived from the very sensitive soft agar migration assay, each of three technical replicates of a given mutant strain was compared to the average migration of the wild-type strain present on the same plates to obtain a ratio of mutant migration relative to that of the wild-type strain. If the mutant migration did not consistently deviate from wild-type migration by more than 15%, the data were included in the supplemental data section. For all mutants, an unpaired *t* test was performed to determine the significance of the deviation of each mutant's migration from that of the average migration of the wild-type strain present on the same three plates. For experiments shown in Fig. 4, 6, and 7, statistical tests included one-way analysis of variance (ANOVA) and Dunnett's test for multiple comparisons. For Fig. 7C, one-way ANOVA and Sidak's multiple-comparison test was used.

SUPPLEMENTAL MATERIAL

Supplemental material is available online only.

SUPPLEMENTAL FILE 1, PDF file, 0.8 MB.

ACKNOWLEDGMENTS

We thank Francis Alonzo for the use of his microplate reader for the growth curve experiments, Patricia Simms for her help with flow cytometry and analysis, Jon Visick for

reviewing the manuscript, and anonymous reviewers for their helpful suggestions. This work was supported by funding from the NIH, R35 GM130355, awarded to K.L.V. We thank past and present members of the lab for their suggestions on this project.

REFERENCES

1. Ross P, Weinhouse H, Aloni Y, Michaeli D, Weinberger-Ohana P, Mayer R, Braun S, de Vroom E, van der Marel GA, van Boom JH, Benziman M. 1987. Regulation of cellulose synthesis in *Acetobacter xylinum* by cyclic diguanylic acid. Nature 325:279–281. https://doi.org/10.1038/325279a0.
2. Romling U, Galperin MY, Gomelsky M. 2013. Cyclic di-GMP: the first 25 years of a universal bacterial second messenger. Microbiol Mol Biol Rev 77:1–52. https://doi.org/10.1128/MMBR.00043-12.
3. Jenal U, Reinders A, Lori C. 2017. Cyclic di-GMP: second messenger extraordinaire. Nat Rev Microbiol 15:271–284. https://doi.org/10.1038/nrmicro.2016.190.
4. Galperin MY, Natale DA, Aravind L, Koonin EV. 1999. A specialized version of the HD hydrolase domain implicated in signal transduction. J Mol Microbiol Biotechnol 1:303–305.
5. Galperin MY, Nikolskaya AN, Koonin EV. 2001. Novel domains of the prokaryotic two-component signal transduction systems. FEMS Microbiol Lett 203:11–21. https://doi.org/10.1111/j.1574-6968.2001.tb10814.x.
6. Ryjenkov DA, Tarutina M, Moskvin OV, Gomelsky M. 2005. Cyclic diguanylate is a ubiquitous signaling molecule in bacteria: insights into biochemistry of the GGDEF protein domain. J Bacteriol 187:1792–1798. https://doi.org/10.1128/JB.187.5.1792-1798.2005.
7. Schmidt AJ, Ryjenkov DA, Gomelsky M. 2005. The ubiquitous protein domain EAL is a cyclic diguanylate-specific phosphodiesterase: enzymatically active and inactive EAL domains. J Bacteriol 187:4774–4781. https://doi.org/10.1128/JB.187.14.4774-4781.2005.
8. Christen M, Christen B, Folcher M, Schauerte A, Jenal U. 2005. Identification and characterization of a cyclic di-GMP-specific phosphodiesterase and its allosteric control by GTP. J Biol Chem 280:30829–30837. https://doi.org/10.1074/jbc.M504429200.
9. Hunter JL, Severin GB, Koestler BJ, Waters CM. 2014. The *Vibrio cholerae* diguanylate cyclase VCA0965 has an AGDEF active site and synthesizes cyclic di-GMP. BMC Microbiol 14:22. https://doi.org/10.1186/1471-2180-14-22.
10. Christen B, Christen M, Paul R, Schmid F, Folcher M, Jenoe P, Meuwly M, Jenal U. 2006. Allosteric control of cyclic di-GMP signaling. J Biol Chem 281:32015–32024. https://doi.org/10.1074/jbc.M603589200.
11. Aravind L, Koonin EV. 1998. The HD domain defines a new superfamily of metal-dependent phosphohydrolases. Trends Biochem Sci 23:469–472. https://doi.org/10.1016/S0968-0004(98)01293-6.
12. Amikam D, Galperin MY. 2006. PilZ domain is part of the bacterial c-di-GMP binding protein. Bioinformatics 22:3–6. https://doi.org/10.1093/bioinformatics/bti739.
13. Chou SH, Galperin MY. 2016. Diversity of cyclic di-GMP-binding proteins and mechanisms. J Bacteriol 198:32–46. https://doi.org/10.1128/JB.00333-15.
14. Ruby EG, Urbanowski M, Campbell J, Dunn A, Faini M, Gunsalus R, Lostroh P, Lupp C, McCann J, Millikan D, Schaefer A, Stabb E, Stevens A, Visick K, Whistler C, Greenberg EP. 2005. Complete genome sequence of *Vibrio fischeri*: a symbiotic bacterium with pathogenic congeners. Proc Natl Acad Sci U S A 102:3004–3009. https://doi.org/10.1073/pnas.0409900102.
15. Mandel MJ, Stabb EV, Ruby EG. 2008. Comparative genomics-based investigation of resequencing targets in *Vibrio fischeri*: focus on point miscalls and artefactual expansions. BMC Genomics 9:138. https://doi.org/10.1186/1471-2164-9-138.
16. Wolfe AJ, Visick KL. 2010. Roles of diguanylate cyclases and phosphodiesterases in motility and biofilm formation in *Vibrio fischeri*. *In* Wolfe AJ, Visick KL (ed), The second messenger cyclic di-GMP. ASM Press, Washington, DC.
17. Visick KL, Stabb EV, Ruby EG. 2021. A lasting symbiosis: how *Vibrio fischeri* finds a squid partner and persists within its natural host. Nat Rev Microbiol 19:654–665. https://doi.org/10.1038/s41579-021-00557-0.
18. Nyholm SV, McFall-Ngai MJ. 2021. A lasting symbiosis: how the Hawaiian bobtail squid finds and keeps its bioluminescent bacterial partner. Nat Rev Microbiol 19:666–679. https://doi.org/10.1038/s41579-021-00567-y.
19. Graf J, Dunlap PV, Ruby EG. 1994. Effect of transposon-induced motility mutations on colonization of the host light organ by *Vibrio fischeri*. J Bacteriol 176:6986–6991. https://doi.org/10.1128/jb.176.22.6986-6991.1994.
20. Millikan DS, Ruby EG. 2003. FlrA, a σ^{54}-dependent transcriptional activator in *Vibrio fischeri*, is required for motility and symbiotic light-organ colonization. J Bacteriol 185:3547–3557. https://doi.org/10.1128/JB.185.12.3547-3557.2003.
21. Wolfe AJ, Millikan DS, Campbell JM, Visick KL. 2004. *Vibrio fischeri* σ^{54} controls motility, biofilm formation, luminescence, and colonization. Appl Environ Microbiol 70:2520–2524. https://doi.org/10.1128/AEM.70.4.2520-2524.2004.
22. Brennan CA, Mandel MJ, Gyllborg MC, Thomasgard KA, Ruby EG. 2013. Genetic determinants of swimming motility in the squid light-organ symbiont *Vibrio fischeri*. Microbiologyopen 2:576–594. https://doi.org/10.1002/mbo3.96.
23. O'Shea TM, Deloney-Marino CR, Shibata S, Aizawa S, Wolfe AJ, Visick KL. 2005. Magnesium promotes flagellation of *Vibrio fischeri*. J Bacteriol 187:2058–2065. https://doi.org/10.1128/JB.187.6.2058-2065.2005.
24. O'Shea TM, Klein AH, Geszvain K, Wolfe AJ, Visick KL. 2006. Diguanylate cyclases control magnesium-dependent motility of *Vibrio fischeri*. J Bacteriol 188:8196–8205. https://doi.org/10.1128/JB.00728-06.
25. Tischler AH, Vanek ME, Peterson N, Visick KL. 2021. Calcium-responsive diguanylate cyclase CasA drives cellulose-dependent biofilm formation and inhibits motility in *Vibrio fischeri*. mBio 12:e0257321. https://doi.org/10.1128/mBio.02573-21.
26. Visick KL, Hodge-Hanson KM, Tischler AH, Bennett AK, Mastrodomenico V. 2018. Tools for rapid genetic engineering of *Vibrio fischeri*. Appl Environ Microbiol 84:e00850-18. https://doi.org/10.1128/AEM.00850-18.
27. Heidelberg JF, Eisen JA, Nelson WC, Clayton RA, Gwinn ML, Dodson RJ, Haft DH, Hickey EK, Peterson JD, Umayam LA, Gill SR, Nelson KE, Read TD, Tettelin H, Richardson D, Ermolaeva MD, Vamathevan J, Bass S, Qin H, Dragoi I, Sellers P, McDonald L, Utterback T, Fleishmann RD, Nierman WC, White O, Salzberg SL, Smith HO, Colwell RR, Mekalanos JJ, Venter JC, Fraser CM. 2000. DNA sequence of both chromosomes of the Cholera pathogen *Vibrio cholerae*. Nature 406:477–483. https://doi.org/10.1038/35020000.
28. Liu X, Beyhan S, Lim B, Linington RG, Yildiz FH. 2010. Identification and characterization of a phosphodiesterase that inversely regulates motility and biofilm formation in *Vibrio cholerae*. J Bacteriol 192:4541–4552. https://doi.org/10.1128/JB.00209-10.
29. Perez-Mendoza D, Coulthurst SJ, Humphris S, Campbell E, Welch M, Toth IK, Salmond GP. 2011. A multi-repeat adhesin of the phytopathogen, *Pectobacterium atrosepticum*, is secreted by a Type I pathway and is subject to complex regulation involving a non-canonical diguanylate cyclase. Mol Microbiol 82:719–733. https://doi.org/10.1111/j.1365-2958.2011.07849.x.
30. Beyhan S, Odell LS, Yildiz FH. 2008. Identification and characterization of cyclic diguanylate signaling systems controlling rugosity in *Vibrio cholerae*. J Bacteriol 190:7392–7405. https://doi.org/10.1128/JB.00564-08.
31. Bellini D, Caly DL, McCarthy Y, Bumann M, An SQ, Dow JM, Ryan RP, Walsh MA. 2014. Crystal structure of an HD-GYP domain cyclic-di-GMP phosphodiesterase reveals an enzyme with a novel trinuclear catalytic iron centre. Mol Microbiol 91:26–38. https://doi.org/10.1111/mmi.12447.
32. Rashid MH, Rajanna C, Ali A, Karaolis DK. 2003. Identification of genes involved in the switch between the smooth and rugose phenotypes of *Vibrio cholerae*. FEMS Microbiol Lett 227:113–119. https://doi.org/10.1016/S0378-1097(03)00657-8.
33. Collins AJ, Smith TJ, Sondermann H, O'Toole GA. 2020. From input to output: the Lap/c-di-GMP biofilm regulatory circuit. Annu Rev Microbiol 74:607–631. https://doi.org/10.1146/annurev-micro-011520-094214.
34. Christensen DG, Marsden AE, Hodge-Hanson K, Essock-Burns T, Visick KL. 2020. LapG mediates biofilm dispersal in *Vibrio fischeri* by controlling maintenance of the VCBS-containing adhesin LapV. Mol Microbiol 114:742–761. https://doi.org/10.1111/mmi.14573.
35. Kitts G, Giglio KM, Zamorano-Sanchez D, Park JH, Townsley L, Cooley RB, Wucher BR, Klose KE, Nadell CD, Yildiz FH, Sondermann H. 2019. A conserved regulatory circuit controls large adhesins in *Vibrio cholerae*. mBio 10. https://doi.org/10.1128/mBio.02822-19.
36. Pickering BS, Smith DR, Watnick PI. 2012. Glucose-specific enzyme IIA has unique binding partners in the *Vibrio cholerae* biofilm. mBio 3:e00228-12. https://doi.org/10.1128/mBio.00228-12.

37. Dial CN, Eichinger SJ, Foxall R, Corcoran CJ, Tischler AH, Bolz RM, Whistler CA, Visick KL. 2021. Quorum sensing and cyclic di-GMP exert control over motility of *Vibrio fischeri* KB2B1. Front Microbiol 12:690459. https://doi.org/10.3389/fmicb.2021.690459.
38. Bassis CM, Visick KL. 2010. The cyclic-di-GMP phosphodiesterase BinA negatively regulates cellulose-containing biofilms in *Vibrio fischeri*. J Bacteriol 192:1269–1278. https://doi.org/10.1128/JB.01048-09.
39. Zamorano-Sanchez D, Xian W, Lee CK, Salinas M, Thongsomboon W, Cegelski L, Wong GCL, Yildiz FH. 2019. Functional specialization in *Vibrio cholerae* diguanylate cyclases: distinct modes of motility suppression and c-di-GMP production. mBio. https://doi.org/10.1128/mBio.00670-19.
40. Zamorano-Sanchez D, Xian W, Lee CK, Salinas M, Thongsomboon W, Cegelski L, Wong GCL, Yildiz FH. 2020. Correction for Zamorano-Sanchez et al., "Functional specialization in *Vibrio cholerae* diguanylate cyclases: distinct modes of motility suppression and c-di-GMP production". mBio 11:e02822-19. https://doi.org/10.1128/mBio.01960-20.
41. Srivastava D, Hsieh ML, Khataokar A, Neiditch MB, Waters CM. 2013. Cyclic di-GMP inhibits *Vibrio cholerae* motility by repressing induction of transcription and inducing extracellular polysaccharide production. Mol Microbiol 90:1262–1276. https://doi.org/10.1111/mmi.12432.
42. Ryjenkov DA, Simm R, Romling U, Gomelsky M. 2006. The PilZ domain is a receptor for the second messenger c-di-GMP. The PilZ domain protein YcgR controls motility in enterobacteria. J Biol Chem 281:30310–30314. https://doi.org/10.1074/jbc.C600179200.
43. Sudarsan N, Lee ER, Weinberg Z, Moy RH, Kim JN, Link KH, Breaker RR. 2008. Riboswitches in eubacteria sense the second messenger cyclic di-GMP. Science 321:411–413. https://doi.org/10.1126/science.1159519.
44. Roelofs KG, Jones CJ, Helman SR, Shang X, Orr MW, Goodson JR, Galperin MY, Yildiz FH, Lee VT. 2015. Systematic identification of cyclic-di-GMP binding proteins in *Vibrio cholerae* reveals a novel class of cyclic-di-GMP-binding ATPases associated with Type II secretion systems. PLoS Pathog 11:e1005232. https://doi.org/10.1371/journal.ppat.1005232.
45. Wang YC, Chin KH, Tu ZL, He J, Jones CJ, Sanchez DZ, Yildiz FH, Galperin MY, Chou SH. 2016. Nucleotide binding by the widespread high-affinity cyclic di-GMP receptor MshEN domain. Nat Commun 7:12481. https://doi.org/10.1038/ncomms12481.
46. Altschul SF, Madden TL, Schäffer AA, Zhang J, Zhang Z, Miller W, Lipman DJ. 1997. Gapped BLAST and PSI-BLAST: a new generation of protein database search programs. Nucleic Acids Res 25:3389–3402. https://doi.org/10.1093/nar/25.17.3389.
47. Marchler-Bauer A, Bo Y, Han L, He J, Lanczycki CJ, Lu S, Chitsaz F, Derbyshire MK, Geer RC, Gonzales NR, Gwadz M, Hurwitz DI, Lu F, Marchler GH, Song JS, Thanki N, Wang Z, Yamashita RA, Zhang D, Zheng C, Geer LY, Bryant SH. 2017. CDD/SPARCLE: functional classification of proteins via subfamily domain architectures. Nucleic Acids Res 45:D200–D203. https://doi.org/10.1093/nar/gkw1129.
48. Marchler-Bauer A, Derbyshire MK, Gonzales NR, Lu S, Chitsaz F, Geer LY, Geer RC, He J, Gwadz M, Hurwitz DI, Lanczycki CJ, Lu F, Marchler GH, Song JS, Thanki N, Wang Z, Yamashita RA, Zhang D, Zheng C, Bryant SH. 2015. CDD: NCBI's conserved domain database. Nucleic Acids Res 43:D222–D226. https://doi.org/10.1093/nar/gku1221.
49. Marchler-Bauer A, Lu S, Anderson JB, Chitsaz F, Derbyshire MK, DeWeese-Scott C, Fong JH, Geer LY, Geer RC, Gonzales NR, Gwadz M, Hurwitz DI, Jackson JD, Ke Z, Lanczycki CJ, Lu F, Marchler GH, Mullokandov M, Omelchenko MV, Robertson CL, Song JS, Thanki N, Yamashita RA, Zhang D, Zhang N, Zheng C, Bryant SH. 2011. CDD: a Conserved Domain Database for the functional annotation of proteins. Nucleic Acids Res 39:D225–D229. https://doi.org/10.1093/nar/gkq1189.
50. Cuthbertson JM, Doyle DA, Sansom MS. 2005. Transmembrane helix prediction: a comparative evaluation and analysis. Protein Eng Des Sel 18:295–308. https://doi.org/10.1093/protein/gzi032.
51. Omasits U, Ahrens CH, Muller S, Wollscheid B. 2014. Protter: interactive protein feature visualization and integration with experimental proteomic data. Bioinformatics 30:884–886. https://doi.org/10.1093/bioinformatics/btt607.
52. Boettcher KJ, Ruby EG. 1990. Depressed light emission by symbiotic *Vibrio fischeri* of the sepiolid squid *Euprymna scolopes*. J Bacteriol 172:3701–3706. https://doi.org/10.1128/jb.172.7.3701-3706.1990.
53. Stabb EV, Ruby EG. 2002. RP4-based plasmids for conjugation between *Escherichia coli* and members of the Vibrionaceae. Methods Enzymol 358:413–426. https://doi.org/10.1016/s0076-6879(02)58106-4.
54. Pollack-Berti A, Wollenberg MS, Ruby EG. 2010. Natural transformation of *Vibrio fischeri* requires *tfoX* and *tfoY*. Environ Microbiol 12:2302–2311. https://doi.org/10.1111/j.1462-2920.2010.02250.x.
55. Brooks JF, 2nd, Gyllborg MC, Cronin DC, Quillin SJ, Mallama CA, Foxall R, Whistler C, Goodman AL, Mandel MJ. 2014. Global discovery of colonization determinants in the squid symbiont *Vibrio fischeri*. Proc Natl Acad Sci U S A 111:17284–17289. https://doi.org/10.1073/pnas.1415957111.
56. Cohen JJ, Eichinger SJ, Witte DA, Cook CJ, Fidopiastis PM, Tepavcevic J, Visick KL. 2021. Control of competence in *Vibrio fischeri*. Appl Environ Microbiol 87. https://doi.org/10.1128/AEM.01962-20.
57. Christensen DG, Tepavcevic J, Visick KL. 2020. Genetic manipulation of *Vibrio fischeri*. Curr Protoc Microbiol 59:e115. https://doi.org/10.1002/cpmc.115.
58. Ho SN, Hunt HD, Horton RM, Pullen JK, Pease LR. 1989. Site-directed mutagenesis by overlap extension using the polymerase chain reaction. Gene 77:51–59. https://doi.org/10.1016/0378-1119(89)90358-2.